

IMPLICATIONS OF A LUNAR FLYBY ENCOUNTER  
WITH EARTH

Thesis for the Degree of Ph. D.  
MICHIGAN STATE UNIVERSITY  
ROBERT JOSEPH MALCUIT  
1973



This is to certify that the

thesis entitled

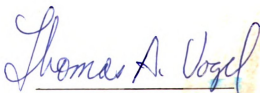
IMPLICATIONS OF A LUNAR FLYBY  
ENCOUNTER WITH EARTH

presented by

Robert Joseph Malcuit

has been accepted towards fulfillment  
of the requirements for

Ph.D. degree in Geology

  
Major professor

Date Jan. 17, 1973

18 + 2 = 20

18 + 2 = 20

18 + 2 = 20

## ABSTRACT

### IMPLICATIONS OF A LUNAR FLYBY ENCOUNTER WITH EARTH

By

Robert Joseph Malcuit

A capture origin of the Moon most likely involved one or more close flyby (non-capture) encounters with Earth prior to the formation of the Moon's current geocentric orbit. Computer simulation modeling of the physical consequences of such encounters suggests that a lunar body with a rigid crust could have been profoundly affected only (1) if the encounter was well within the weightlessness limit of the Earth-Moon System (a limit located at  $1.63 R_e$  (Earth radii), measured from center of Moon) and (2) if the lunar upper mantle could yield large quantities of magma over the very short period of time (20-30 min.) while within this weightlessness limit. Under the above conditions, a substantial mass of lunar crust and upper mantle material could be pulled from the lunar surface and interior by Earth's gravity and either escape from the Moon or fall back onto the lunar surface.

Under ideal conditions and in the case of a non-spinning Moon, all launch and backfall positions of lunar



material affected by the encounter would be located along a great circle on the lunar surface here called the encounter plane. In a more realistic case of a spinning Moon, a curvilinear pattern is produced.

The large circular maria--Oriental, Imbrium, Serenitatis, Crisium, and Smythii--describe a curvilinear pattern that lies close to a lunar great circle. If Imbrium, Serenitatis, Crisium, and Smythii are interpreted as impact sites of large backfallen bodies of material derived from the lunar crust and upper mantle, then there are two possible eruptive launch regions: (1) Mare Oriental and (2) a region of Oceanus Procellarum located between Mare Oriental and Mare Imbrium.

One possible solution for generation of the maria pattern requires an encounter velocity of 6.0 km/sec and a pericenter (closest approach) distance of  $1.3 R_e$ . Under these conditions, all material for the large circular maria could be derived from the Oceanus Procellarum source region and that material derived from the Mare Oriental region would escape from the Moon. The presence of primitive crust between the two features interpreted as eruptive launch regions implies that the lunar crust was rigid enough at encounter time to prevent continuous launching of lunar subsurface material during the launch phase.

The large circular maria--Imbrium, Serenitatis, Crisium, and Smythii--are interpreted as impact locations of large spheroidal basaltic masses which were launched

from the Oceanus Procellarum eruptive region and transported above the lunar surface by interaction of Earth and Moon gravitational forces to their respective impact positions during the launch and backfall phases of a single lunar flyby encounter. Upon impact these spheroidal masses simultaneously bent down a pliable lunar crust and collapsed upon themselves to form large circular lava lakes (maria) on the lunar surface. The maria surfaces were subsequently cratered by (1) lunar material which was launched early in the encounter and did not escape from the Moon and (2) meteoritic material from space.

Interpretation of the large circular maria and associated features as flyby encounter "scars" implies that the Moon was once an independent planet (asteroid) in a heliocentric orbit that was perturbed by Jupiter, over a period of time, into an Earth-crossing orbit. The, after a series of flyby encounters with Earth, with at least one that was well within the weightlessness limit, the asteroid-Moon was captured into a geocentric orbit.

IMPLICATIONS OF A LUNAR FLYBY  
ENCOUNTER WITH EARTH

By

Robert Joseph Malcuit

A THESIS

Submitted to  
Michigan State University  
in partial fulfillment of the requirements  
for the degree of

DOCTOR OF PHILOSOPHY

Department of Geology

1973

920250

## ACKNOWLEDGEMENTS

I wish to thank Dr. T. A. Vogel for valuable advice and assistance in preparation of this thesis and for critically reading the manuscript. I am grateful to Dr. T. R. Stoeckley, Department of Astronomy, Michigan State University, for the use of his computer program and for his assistance in many phases of this study. I am indebted to Gary Byerly for instructions in the use of the computer facilities and for many valuable discussions of various thesis-related topics. I wish to express thanks to Dr. R. Ehrlich, Dr. C. M. Spooner, Dr. H. F. Bennett, and Dr. H. B. Stonehouse for valuable suggestions and discussions. Other faculty members and students of the Department of Geology, Michigan State University, provided helpful advice and discussion.

Finally, I am grateful for the support of a Humble Oil Company Fellowship while in graduate school at Michigan State University and to the Departments of Geology and Astronomy, Michigan State University, for computer time.

TABLE OF CONTENTS

	Page
ACKNOWLEDGEMENTS . . . . .	ii
LIST OF FIGURES . . . . .	iv
LIST OF PLATES . . . . .	v
 Chapter	
I. INTRODUCTION . . . . .	1
II. PRESENTATION OF MODEL AND COMPARISON TO ROCK PATTERNS ON MOON AND EARTH . . . . .	4
General Statement . . . . .	4
Assumptions of Pre-encounter Conditions of Earth and Moon . . . . .	4
The Flyby Encounter Episode . . . . .	5
Possible Interactions Between Earth and Asteroid-Moon . . . . .	5
Possible Consequences of an Encounter Within the Weightlessness Limit and and Comparison to Rock Patterns on Moon and Earth . . . . .	9
III. IMPLICATIONS FOR THE HISTORY OF THE EARTH-MOON ASSOCIATION . . . . .	44
IV. SUMMARY AND CONCLUSIONS . . . . .	47
REFERENCES CITED . . . . .	49

## LIST OF FIGURES

Figure		Page
1.	Diagram showing geometrical similarities and differences between classical Roche limit and weightlessness limit for the case of the Earth and Moon . . . . .	7
2.	Scale diagram showing path of Moon relative to Earth within the interval +10 to -12 $R_e$ during a flyby encounter . . . . .	10
3.	Cross-sectional diagrams of Moon (a-f) showing sequence of events at positions A-F, respectively, in Figure 2 . . . . .	14
4.	Composite diagram showing trajectories, flight times, and impact sites ( $C_m-C_e$ ) of bodies launched during the encounter in Figure 3 . . . . .	17
5.	Series of map-view diagrams showing the effects of lunar rotation (spin) on the surface rock patterns that could be generated during a flyby encounter featuring only 5 closely spaced launch sites . . . . .	19
6.	Geometrical comparison of model and actual lunar surface patterns . . . . .	28
7.	Map-view diagrams of Moon showing the locations of major surface features . . . . .	32
8.	Time scale for the evolution of the Earth-Moon System . . . . .	46

LIST OF PLATES

Plate		Page
1.	Photograph of front side of Moon . . . . .	24
2.	Photograph of eastern limb of Moon . . . . .	25
3.	Photograph of the Mare Oriental-western Oceanus Procellarum region . . . . .	26
4.	Photograph of typical example of flooded terrae . . . . .	37
5.	Photograph of Mare Crisium, a typical circular mare, showing raised rim, flooded terrae on edge, and various stages in the development of secondary (post-mare) cratering . . . . .	39

. . . in the entire solar system the earth-moon association is completely unique, and the recognized difficulties in all proposed modes of origin seem to demand an unusual solution.

Ralph Baldwin (1966)



## CHAPTER I

### INTRODUCTION

Theories of the origin of the Earth-Moon System assume either that both bodies have coexisted since their formation or that the Moon was captured at a later time. Conditions necessary for capture are limited and, as discussed below, probably involved one or more close non-capture encounters previous to the formation of the Moon's current circumterrestrial orbit.

If a close flyby (non-capture) encounter occurred, both bodies would have been severely affected by their interacting gravitational fields. The consequences of such an encounter are a function of the encounter velocity, the closeness of approach, the physical state of the bodies, and the state of their geochemical differentiation. Enough data now exist to estimate the conditions under which profound effects might have occurred. The purpose of this paper is to investigate the theoretical consequences of a close encounter of the Earth and Moon to see if the data from both bodies are consistent with such an encounter model.

Cloud (1968) first suggested that an Earth-Moon encounter may have played a significant role in the early

evolution of both bodies, and he accurately predicted the age of basalts from Mare Tranquillitatis to be about 3.6 billion years. His prediction was based on the assumption that a major thermal episode on Earth was related to the development of maria on the Moon and that both of these events were caused simultaneously by a near approach of the Moon to the Earth. Cloud proposed that the Moon was captured by the Earth at this time in a prograde orbit in a manner described by Singer (1968). However, if the Moon was once an independent planet in heliocentric orbit, it is probable that flyby encounters occurred prior to lunar capture, since Gerstenkorn (1969) has shown that encounters with initial velocities greater than 1 km/sec probably would not result in capture.

The central theme of this paper is that the mare distribution pattern on the Moon and the occurrence of a major thermal episode on Earth are consistent with a flyby encounter of the Moon within the weightlessness limit\* of the Earth-Moon System.

More specifically, the major purpose of this work is:

1. To investigate the consequences of close lunar flyby encounters with Earth on the exterior rock patterns of both bodies under various physical constraints.

---

\*A physical limit, newly defined later in this paper, which is located much nearer to the Earth's surface than the classical Roche limit.

2. To demonstrate that the time-rock patterns on the Moon and the Earth are consistent with the theoretical patterns which could be generated by such encounters.

3. To discuss some of the implications that the flyby encounter model has for the geologic history of the Earth and Moon.

In general, this work is limited to the study of possible Earth-Moon interactions up to the point of lunar capture and is not concerned with the details of the capture process or the subsequent orbital evolution of the Moon in geocentric orbit. The main purpose here is to show that the flyby encounter model is a viable one and is consistent with the major geologic-petrologic patterns of both planets at our present level of knowledge. (For a general review of proposed hypotheses of the origin of the Earth-Moon System, recent reviews have been published by Hinners (1971), Kaula (1971), and Lowman (1972).)

CHAPTER II  
PRESENTATION OF MODEL AND COMPARISON TO ROCK  
PATTERNS ON MOON AND EARTH

General Statement

A flyby encounter model can be examined in three stages: the pre-encounter period, the encounter episode, and the post-encounter period. For each stage, expected characteristic rock patterns resulting will be compared to the actual rock patterns on Moon and Earth.

Assumptions of Pre-encounter Conditions  
of Earth and Moon

Assumptions for this model are very general and pertain mainly to pre-encounter orbital characteristics and planetary body conditions of the Earth and Moon. The Earth's planetary orbit is assumed to have been stable (essentially unchanged) since culmination of the accretion process. The primitive (pre-encounter) Earth is assumed to have had a thinner lithosphere and a thicker, warmer upper mantle than it does today. These conditions are consistent with numerous primitive Earth models such as those proposed by Ringwood (1960, 1966, 1969), Birch (1965), Hanks and Anderson (1969), Alfvén and Arrhenius (1970a,b), and others.

The primitive Moon is assumed to have been an independent planet in heliocentric orbit. A likely place for such an orbit is in the Asteroid Belt. Any lunar body model resulting in an anorthositic crust and a gabbroic upper mantle is satisfactory. Such models have been proposed or discussed by Smith et al. (1970), Sonnet et al. (1971), Wood (1972), and others.

### The Flyby Encounter Episode

#### Possible Interactions Between Earth and Asteroid-Moon

There are three general types of encounters: capture encounters, collision encounters, and flyby encounters. Only the latter will be analyzed in this study. The underlying concepts concerning the location of the classical Roche limit for the Earth-Moon System must be discussed before the probable effects of flyby encounters can be understood. The Roche limit is defined in fluid dynamic terms as the locus of points about a planet at which a fluid satellite becomes an unstable ellipsoid and begins to disintegrate by necking (Darwin, 1898; Roskol, 1966). For the Earth-Moon System this limit is located about  $2.89 R_e$  (Earth radii) from the center of the Earth, measured from the center of the Earth to the center of the Moon ( $C_m - C_e$ ). But for solid bodies such as the Moon, which are much less deformable than fluid bodies, this limit has very little meaning. However, another limit which is located even

closer to the Earth does have physical meaning. This inner limit is defined, in strictly gravitational terms, as the center-to-center distance between the Earth and the Moon at which weightlessness occurs at the subearth point on the lunar surface (that point located nearest to Earth along the line connecting Earth and Moon centers). In other words, it is the locus of points at which Earth gravity will overcome lunar gravity plus the acceleration of the Moon toward the Earth at the subearth point on the lunar surface. For example, a particle which is unattached to the lunar surface would, beyond this limit, lift off the lunar surface and be accelerated toward the Earth, regardless of the motion of the Moon, i.e., flyby encounter, circular orbit, elliptical orbit, etc. This weightlessness limit is located at about  $1.63 R_e (C_m - C_e)$ . The subearth point for this limit is located about  $1.36 R_e$  from the center of the Earth. Mathematically, the weightlessness limit (W limit) is defined as:

$$\frac{GM_e}{r^2} = \frac{GM_e}{(r-R_m)^2} - \frac{GM_m}{R_m^2}$$

where  $G$  = gravitational constant;  $M_e$  = mass of Earth;  $M_m$  = mass of Moon;  $r$  = distance of separation of Earth and Moon centers; and  $R_m$  = radius of Moon.

Figure 1 demonstrates some geometrical similarities and differences between the classical Roche limit and the

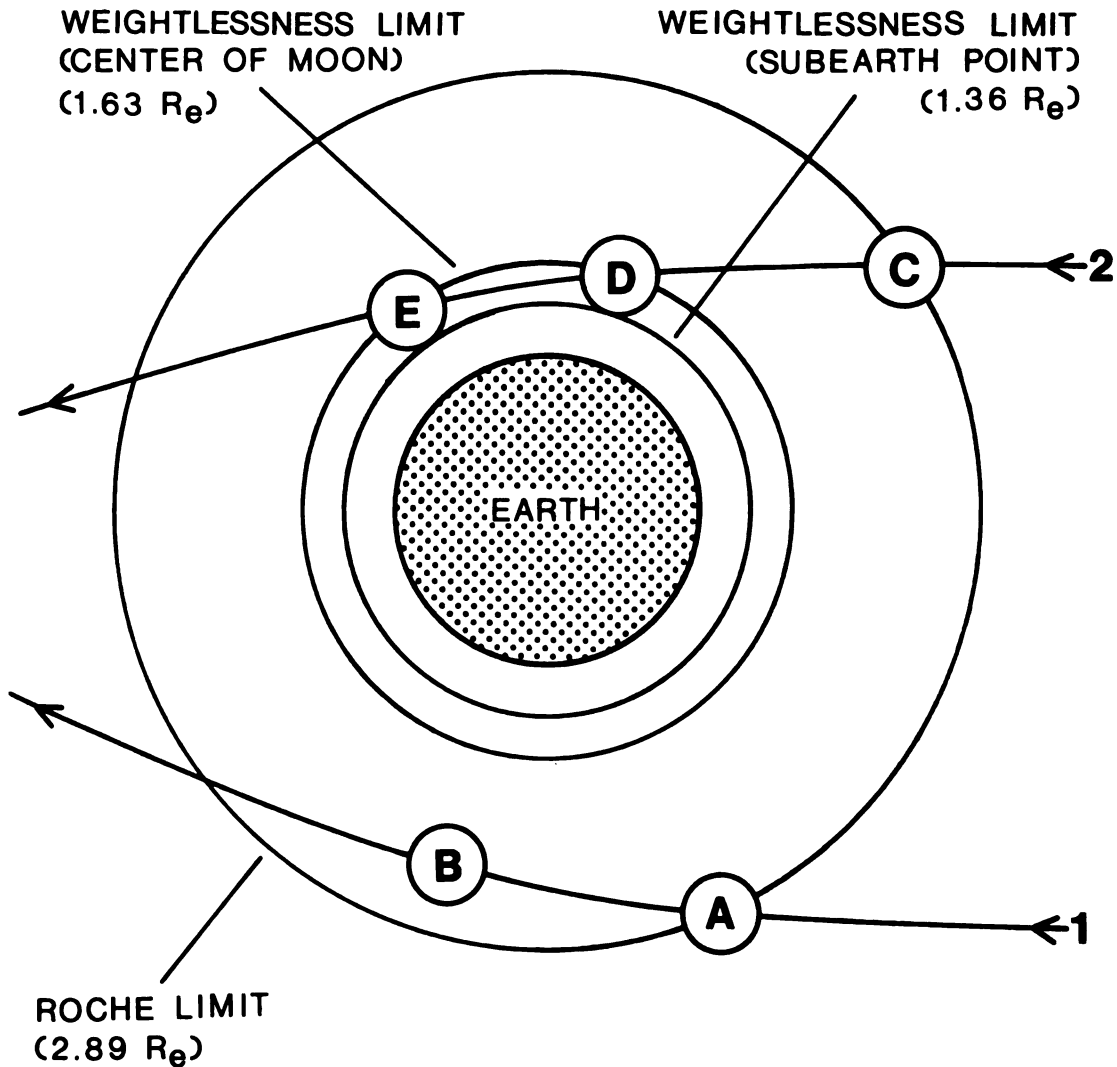


Figure 1.--Diagram showing geometrical similarities and differences between classical Roche limit and weightlessness limit for the case of the Earth and Moon. Both limits describe a theoretical, equipotential surface surrounding the Earth. However, only the weightlessness limit is significant in the case of a solid satellite during a flyby encounter. Trajectories 1 and 2 show paths of the Moon on two separate flyby encounters. In case 1, no point at the lunar surface would experience weightlessness even though it is well within the classical Roche limit; the Moon would undergo only tidal deformation. In case 2, the Moon would experience weightlessness on a portion of its surface nearest the Earth between positions D and E.

weightlessness limit. These differences are extremely important when considering what could happen during very close flyby encounters.

Figure 1 also shows two general types of high velocity, flyby encounters which are of principle interest here. They are: (1) the Moon approaches the Earth but does not penetrate the W limit (trajectory 1) and (2) the Moon approaches the Earth and traverses a section within the W limit (trajectory 2). As Figure 1 shows, the most obvious effect of flyby encounters is deflection of the lunar orbital path. Widespread internal deformation and heating of both bodies by tidal friction would also result. The magnitude of the deformation and heating would be determined by the velocity of the encounter, the distance of separation at closest approach, and the physical state of the outer regions of the two planets.

The trajectory of the Moon during a flyby encounter with Earth can be considered as a classical Newtonian two-body problem and is dependent on two variables: the impact parameter,  $I$ , and the encounter velocity,  $V_0$ . (The masses of the two bodies are considered invariant during the encounter.) Since the critical concern here is with the distance of closest approach (pericenter radius),  $r_p$ , during an encounter, it can be used in place of the impact parameter. Then, from these two parameters,  $V_0$  and  $r_p$ , three other important parameters can be obtained with the following equations:



$$v_p^2 = v_o^2 + \frac{2GM_e}{r_p}$$

$$I = \frac{v_p r_p}{v_o},$$

and

$$\cot \frac{\theta}{2} = \frac{v_o^2 I}{GM_e},$$

where  $v_p$  = velocity of Moon at closest approach (pericenter);  $v_o$  = encounter velocity (velocity at infinity);  $G$  = gravitational constant;  $M_e$  = mass of Earth;  $r_p$  = distance at closest approach (pericenter radius);  $I$  = impact parameter; and  $\theta$  = angle of deflection. From these relationships, the geometry of an encounter can be constructed and its possible consequences analyzed.

#### Possible Consequences of an Encounter Within the Weightlessness Limit and Comparison to Rock Patterns on Moon and Earth

##### General Statement

The possible effects of lunar flyby encounters with Earth can be isolated by simulation models so that real geologic-petrologic features on the Moon and Earth can be compared to model features. Figure 2 shows the general aspects of such an encounter model. In this example  $v_o = 6.0$  km/sec and  $r_p = 1.4 R_e$ . Both of these values are considered central values for a flyby encounter within the W limit for the case of a lunar body from an asteroidal

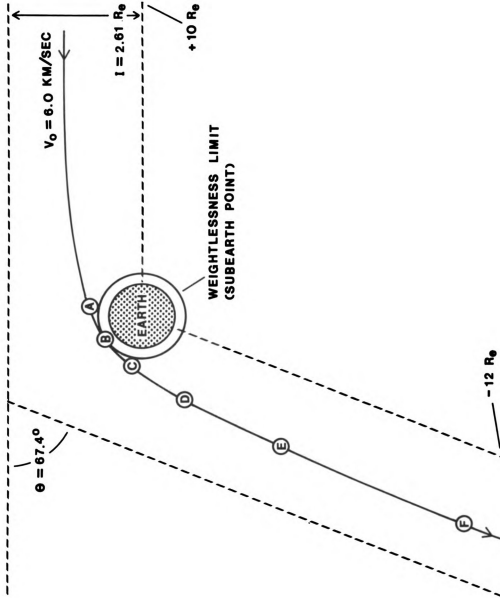


Figure 2.--Scale diagram showing path of Moon relative to Earth within the interval  $+10$  to  $-12 R_E$  during a flyby encounter.  $V_0 = 6.0 \text{ km/sec}$ ;  $r = 1.4 R_E$ ; other encounter parameter values are shown on the diagram. Positions of Moon (A-F) represent stages of the encounter which are discussed in the text.

source. This encounter velocity corresponds to an asteroid-Moon with an aphelion at 2.8 A. U. and a perihelion just touching Earth's orbit.

### Effects on the Moon

#### Model Effects on the Moon

A flyby encounter with the above physical parameters can be divided into four phases: pre-launch, launch, back-fall, and post-backfall. The broad outline of events that could occur during such an encounter can be discussed with the aid of Figure 2. Then, a more detailed analysis of an encounter, based on a computer simulation model, will be presented.

During the pre-launch phase, from several hundred Earth radii to the W limit (Figure 2, position A), a spinning Moon comes under the influence of the Earth's gravitational field. The magnitude of lithospheric tides raised on each body depends on the deformability of the planetary crusts and upper mantles at encounter time. This lithospheric tidal deformation causes heat generation within the planetary interiors.

Since the effects of an encounter on the two bodies is strongly dependent on the state of the lunar upper mantle, broad limits on its physical state can be used to place broad limits on the encounter effects. Two important limiting conditions for the lunar upper mantle at encounter time are: (1) it is entirely crystalline and (2) it contains a

zone of molten lunar basalt beneath a thin crust. For modeling purposes the latter is assumed first, but other possibilities will be considered later in this paper. At encounter time, then, a significant mass of molten lunar basalt is assumed available within the lunar upper mantle as the Moon penetrates the W limit. The anorthositic crust overlying this molten lunar mantle zone is severely kneaded by tidal friction processes as the Moon approaches the W limit and throughout the encounter.

In this model, the launch phase begins as the model Moon enters the W limit (position A) and ends as the Moon departs from the W limit (position C). During the launch phase, available lunar crust and mantle material is launched from the lunar surface under the influence of the Earth's gravity. The locus of launch sites is situated along the trace of the line connecting the Earth and Moon centers. In the case of a non-spinning Moon, this trace lies on a lunar great circle, the encounter plane. In the general case of a spinning Moon, this trace forms a curvilinear pattern on the lunar surface. The details of the physical and chemical characteristics of the launched material, as well as the style of its transport (as spheroids, gas-charged clouds, etc.) depends on a great many variables (volatile content, viscosity, etc.) the analysis of which is beyond the scope of this paper. However, assuming

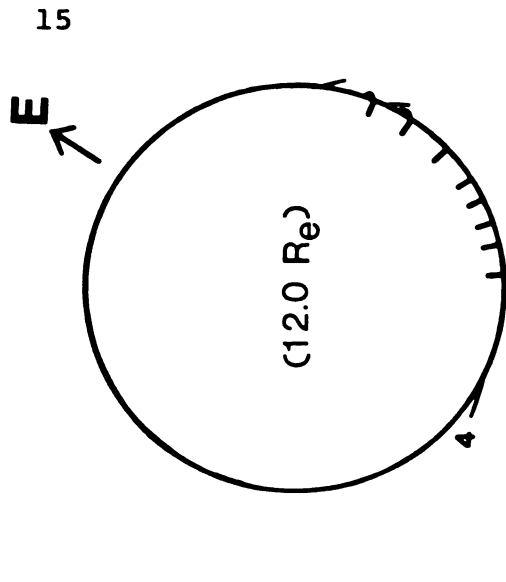
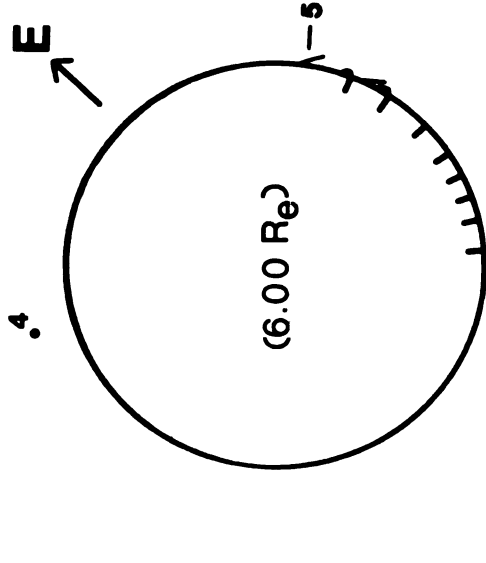
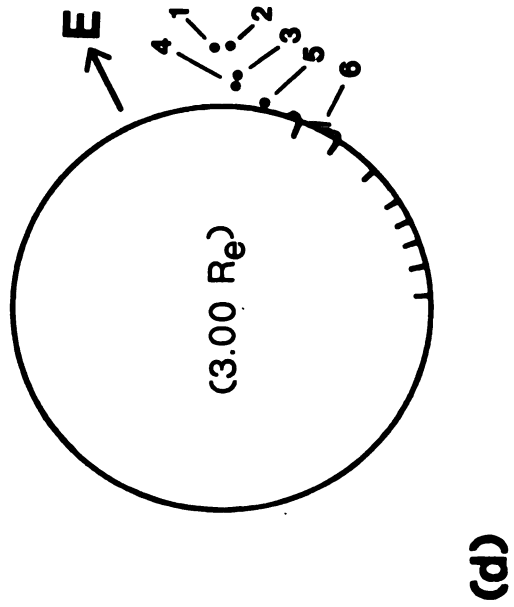
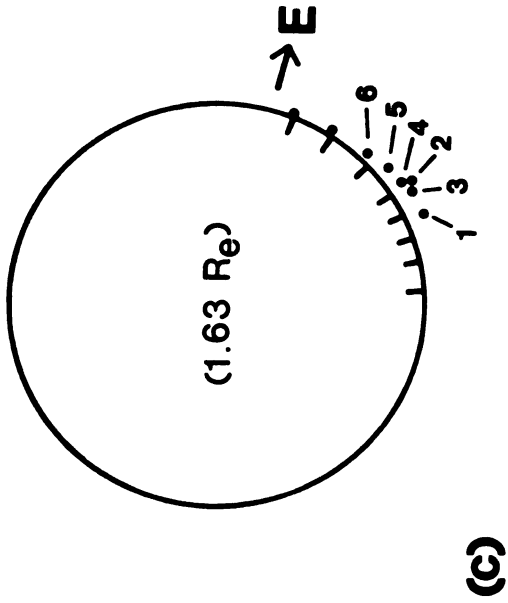
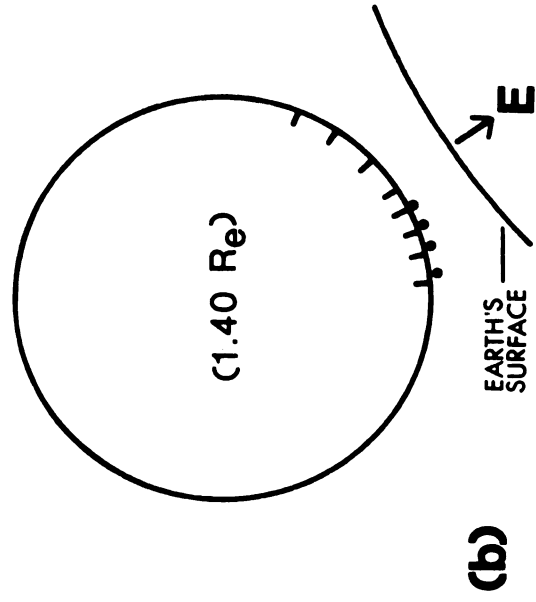
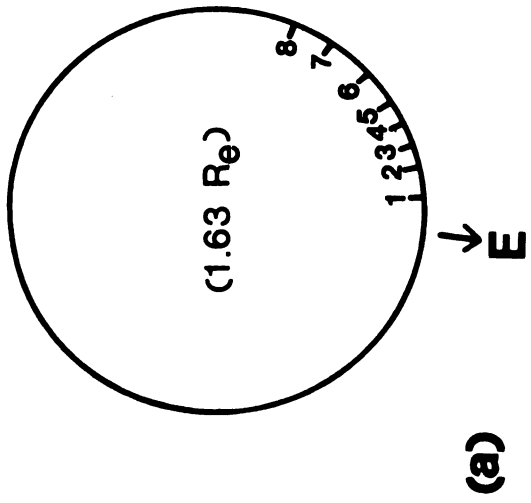
material is available, the launch phase ends with a mass of lunar upper mantle and crustal material suspended above the lunar surface.

As the Moon departs from the W limit, the launch phase ends and the backfall phase begins. During the latter, all spaceborne lunar material that did not attain escape velocity during the encounter eventually returns to the Moon. In general, the last material to be launched from the lunar surface is the first to fall back onto it; the first material launched, provided that it does not escape, falls back last. The general order of backfall (impact), then, is the reverse of that of launch. The backfall stage continues until all lunar material launched during the encounter, except that which escaped from the Moon, returns.

During the post-backfall phase, the Moon is bombarded by meteoritic space particles of low flux density as it was prior to the encounter.

To add precision to the generalized conceptual model presented above, a computer simulation model was constructed using the encounter parameters in Figure 2 and a non-spinning Moon. First, a numerical model was obtained for a two-body encounter between Earth and Moon. Then, three-body models were used to obtain data for the gravitational interaction of the Earth and Moon on bodies launched from various subearth points of the lunar surface. (The trajectories of the particles were calculated numerically on the Michigan State University CDC 6500 computer using a fourth-order

Figure 3.--Cross-sectional diagrams of Moon (a-f) showing sequence of events at positions A-F, respectively, in Figure 2. (a) at W limit entrance; (b) at closest approach; (c) at W limit exit; (d) at -3 Re; (e) at -6 Re; and (f) at -12 Re (C-C). Numbers on bodies correspond to launch site numbers. Short curved lines mark positions and angles of impact of backfalling bodies.



Runga-Kutta integration for three bodies, Earth, Moon, and particle, in three dimensions.)

Using this model, particles 1-8 (Figure 3a) were released from launch sites 1-8, respectively. These bodies were released at the subearth point when the line connecting Earth and Moon centers intersected their positions at the lunar surface. The bodies can be thought of as representing either boulders or basaltic spheroidal masses. As long as their mass is small relative to the Moon (less than  $10^{22}$  gm.), it is negligible in calculating trajectories. Figure 3b shows the approximate locations of the individual bodies at the distance of closest approach,  $r_p$ ; Figure 3c shows their positions at the end of the launch phase. The time elapsed during the launch phase is about 24 minutes.

The backfall phase of the simulation model starts with Figure 3c. Figure 3d shows the approximate locations of the launched bodies at  $3 R_e$ . At this position of the Moon, bodies 8, 7, and 6 (the last three bodies to be launched) have already impacted, and body 5 is very near to impact. In Figure 3e only body 5 is added to the impact list, but the other bodies have scattered considerably. At  $12 R_e$  (Figure 3f) body 4 has returned, but bodies 1, 2, and 3 are still spaceborne.

Figure 4 shows a composite of launch sites, trajectories, impact sites, flight times, and impact locations of bodies 1-8. Considering just the flight times and impact locations of these bodies, some generalizations can be made



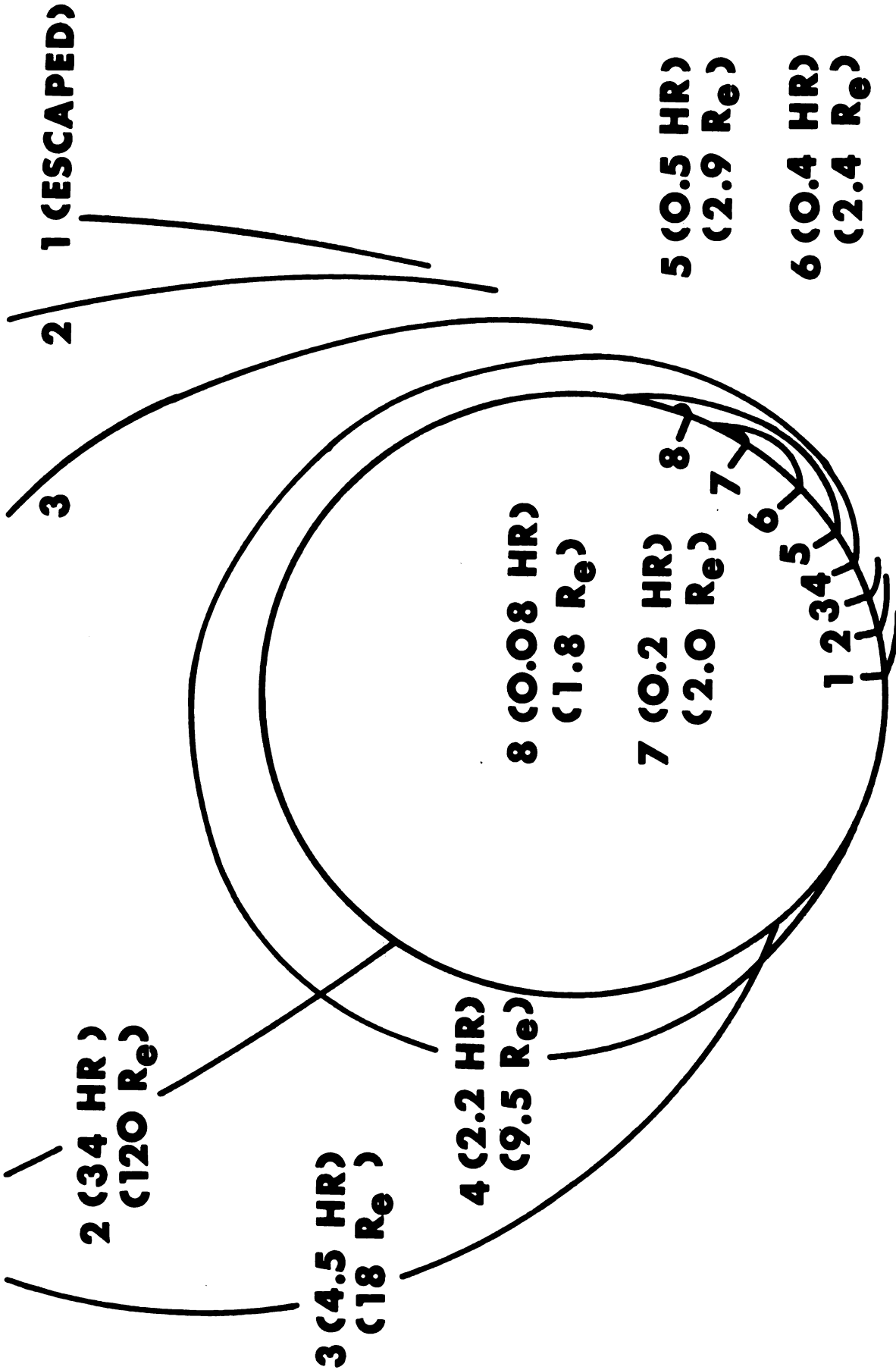


Figure 4.--Composite diagram showing trajectories, flight time, and impact sites ( $C_m - C_e$ ) of bodies launched during the encounter in Figure 3.

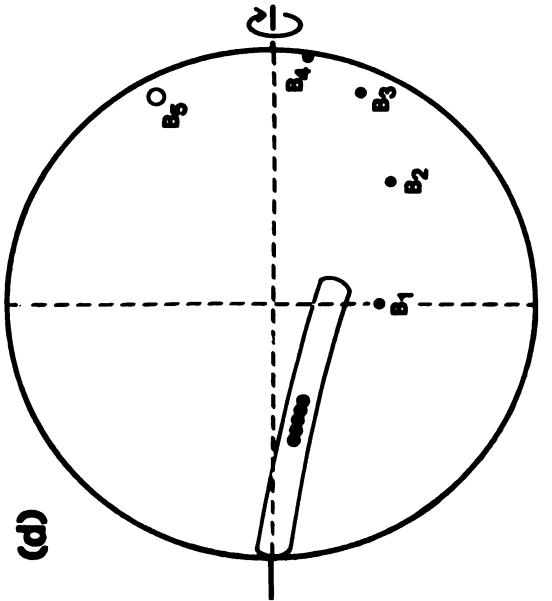
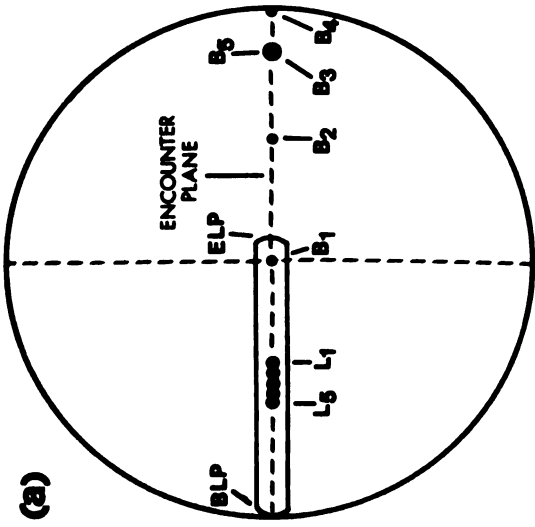
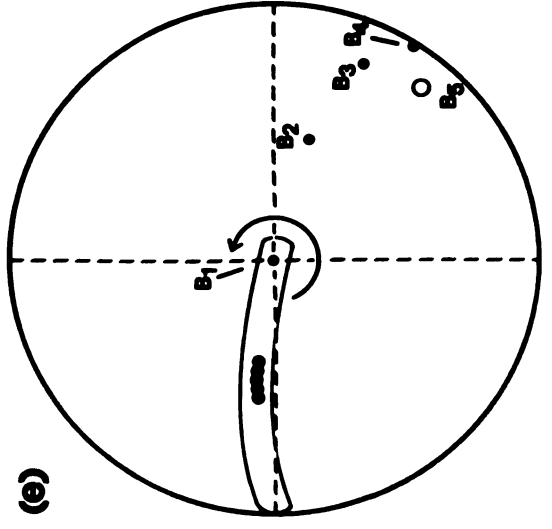
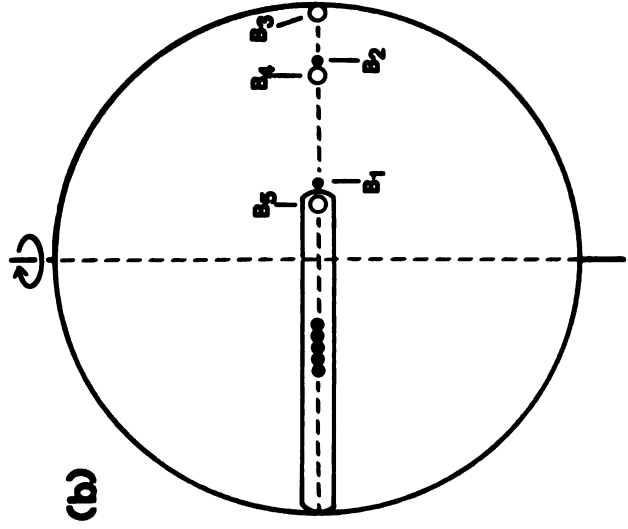
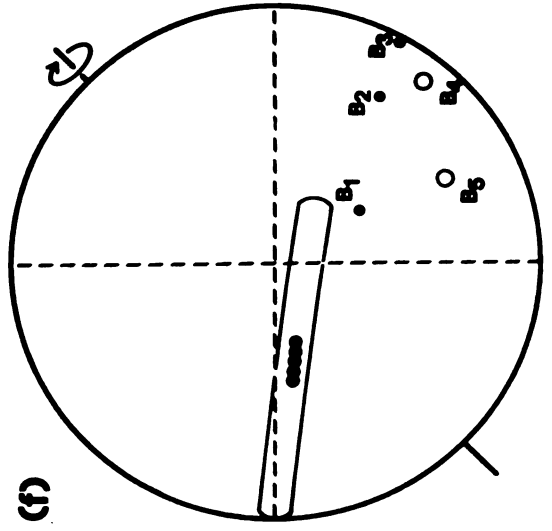
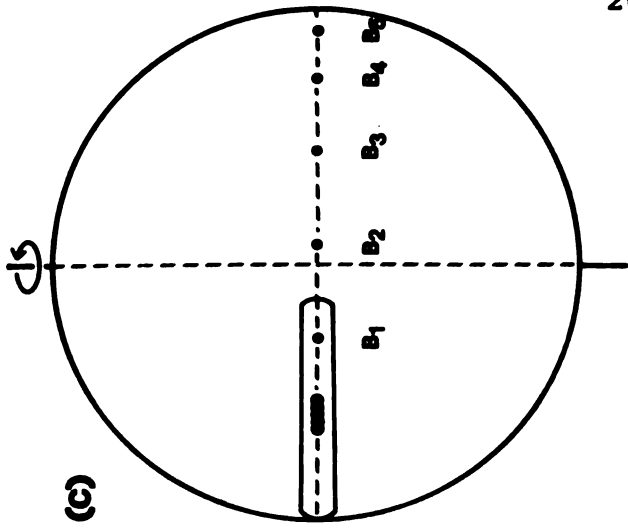
concerning the trajectories of bodies released from intermediate launch sites:

1. Much of the material launched before body 2 escaped permanently from the Moon.
2. A relatively large range of flight times and impact locations exists for bodies launched between launch points 4 and 5 compared to numerical values of these quantities for bodies launched between points 5 and 7.
3. Material launched after body 7 is displaced only a short (insignificant) distance compared to the displacement of other bodies.

A more general model for flyby encounters must include the effects of lunar rotation (spin) during the encounter. Figure 5 shows map patterns of simulated encounters on orthographic projections (which are identical to the lunar grid). The figure shows examples of encounters with limited launch sites for both the special case of a non-spinning Moon and several cases of rotating Moons. Positions of launch and backfall features are based on a numerical simulation model similar to that shown in Figure 3 in which trajectories were calculated for bodies released from closely spaced launch sites.

In the non-spinning case (Figure 5a) all launch and backfall features are confined to the encounter plane which is the plane of the diagrams in Figures 2 and 3.

Figure 5.--Series of map-view diagrams showing the effects of lunar rotation (spin) on the surface rock patterns that could be generated during a flyby encounter featuring only 5 closely spaced launch sites. The BLP (begin launch phase) position, located where the lunar surface first enters the weightlessness limit, is always restored to the left limb of the orthographic projection (same as the lunar grid). The dashed lines represent the lunar equator and the lunar prime meridian of the lunar grid. The encounter plane is always horizontal. Lunar spin rate is constant - 10 hr/day ( $36^\circ/\text{hr}$ ) in all spinning models (b-f). ELP (end launch phase) is located where the lunar surface exits from the W limit. The solid black dots within the launch region (L1-5) mark the launch sites of back-falling bodies B1-5, respectively. Small solid circles mark front-side backfall sites and open circles mark backside backfall sites. In the non-spinning case (a) B1-5 are located approximately  $0^\circ$ ,  $30^\circ$ ,  $60^\circ$ ,  $90^\circ$ , and  $120^\circ$ , respectively, to the right of center of the projection. The approximate flight times of the bodies are 0.5 hr., 0.7 hr., 0.9 hr., 1.1 hr., and 1.3 hr., respectively. Launch sites, flight times, and backfall sites for the five bodies are based on an encounter model similar to that presented in Figure 3 but containing several closely spaced launch sites. Encounter parameters are  $V_0 = 6.0 \text{ km/sec}$  and  $r_p = 1.3 R_e$ . The effects of reducing  $r_p$  by 0.1  $R_e$  will be discussed later in this paper.



Figures 5b and c show cases where the spin plane coincides with the encounter plane. Here the launch and backfall features are concentrated or dispersed along the encounter plane depending on the direction and rate of spin.

Figure 5d and e demonstrate cases where the spin plane is oriented perpendicular to the encounter plane. Here the pattern is deflected to the top or bottom of the projection depending on the rate and direction of spin.

Figure 5f illustrates an intermediate case where the spin plane is oriented at  $45^\circ$  to the encounter plane. Here the pattern is deflected to the lower right of the diagram. This pattern appears relevant because it closely resembles the pattern of prominent features on the actual lunar surface.

In the model presented above, a significant mass of molten basalt is present within the lunar upper mantle. Other conditions are possible and can now be evaluated. These are: (1) the lunar interior is cold and could yield no magma during the encounter and (2) the lunar interior is warm but magma is not readily available within the lunar upper mantle at the time of penetration of the W limit. In the first case, the launch phase features would consist merely of loose debris that would lift off the lunar surface, travel some distance in space, and then fall back onto the lunar surface in the reverse order of liftoff. The surface rock pattern, in this case, would be relatively undisturbed.

In case 2, there would occur a composite of features that characterize the two limiting cases discussed before. In this intermediate situation, some model launch phase features may be missing and primitive, unbreached lunar crust may exist in their positions. These can be considered as empty launch sites. Any launch phase irregularities would be expected to be reflected in the backfall pattern, a principle well demonstrated in the limited launch model in Figure 5. The actual lunar surface pattern can now be compared to the theoretical encounter model pattern to see if this model is viable.

#### Comparison to Real Rock Patterns on the Moon

Delineation of the Primary Pattern and its Geometric and Petrologic Implications.--A flyby encounter, involving deep penetration of the weightlessness limit by a "warm" Moon, would result in hypervolcanic eruption at the sub-earth point and subsequent displacement of lunar crust and mantle material. Some of this material would be pulled from the lunar surface and interior and permanently escape from the Moon; other material would be scattered upon the lunar surface along a straight or curvilinear line with one end terminating at the volcanic source region of first eruption. The launch and backfall patterns, if discernible, can be used to place some limits on the physical parameters of the encounter.

The backfall pattern would be controlled mainly by the type of material launched and the style of launchings. For example, if material was launched continuously, then a continuous pattern of backfall features would occur. Similarly, if the material was launched discontinuously and featured the formation of basaltic spheroids, then the backfall pattern would mark the sites of impact of these discrete bodies of material upon the lunar surface.

The maria pattern is consistent with the discontinuous launch model and comprises a strikingly linear trend of large circular maria which can be at least traced from Mare Oriental to Mare Smythii. The complete series is: Mare Oriental, Mare Imbrium, Mare Serenitatis, Mare Crisium, and Mare Smythii (Plate 1). These features lie essentially along a great circle on the lunar surface. The backside feature, Mare Tsiolkovsky, also lies close to this trend (Plate 2). If such a pattern is the product of a close encounter, then it is the locus of subearth points during the launch and backfall phases of that particular encounter.

To the west of Mare Imbrium (Plate 1) occurs the relatively featureless region of Oceanus Procellarum, an irregular mare. From photographic evidence, it is doubtful whether or not this area could have been an eruptive launch center. However, to the southwest of Oceanus Procellarum, on the western limb of the Moon, is Mare Oriental (Plate 3), a circular basin that is relatively unfilled with mare basalts. From photographs, this feature can be interpreted

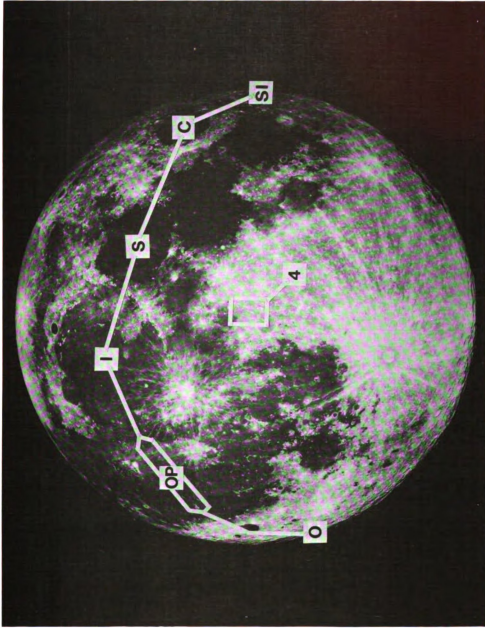


Plate 1.--Photograph of front side of Moon. Major pattern features: O = Oceanus Procellarum; I = Mare Imbrium; S = Mare Serenitatis; C = Mare Crisium; SI = Mare Crisium; SI = Mare Smythii. Solid white line connects inferred eruptive launch regions and backfall phase features and encloses inferred eruptive launch region within Oceanus Procellarum. Number 4 indicates location of Plate 4. (Hale Observatory Photo.)



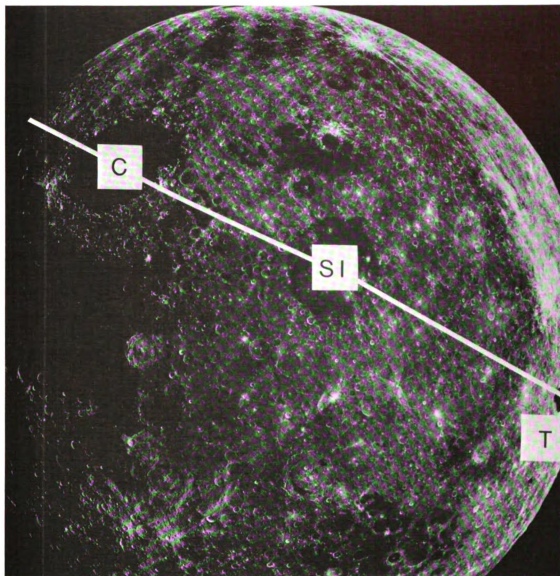


Plate 2.--Photograph of eastern limb of Moon. C = Mare Crisium; SI = Mare Smythii; T = Mare Tsiolkovsky; solid white line connects inferred major features of backfall phase. (Apollo 8-14-2485.)

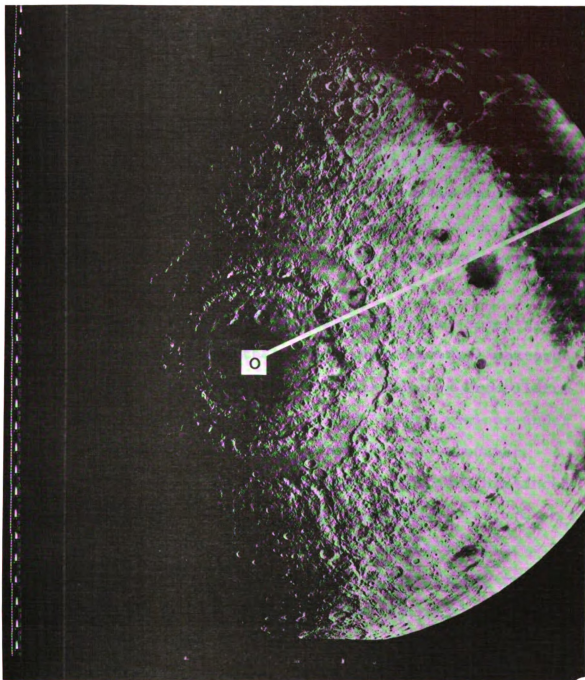


Plate 3.--Photograph of the Mare Oriental-western Oceanus Procellarum region. O = Mare Oriental, an inferred eruptive launch region. The solid white line connects Mare Oriental with a second inferred eruptive launch region, Oceanus Procellarum. (Lunar Orbiter Photograph IV 187M).

as a huge volcanic cone that formed at the culmination of gigantic lunar tides that would have affected the Moon during a very close approach to Earth. Thus, if the model is correct, the Mare Oriental region was the location of a hypervolcanic eruptive launch center.

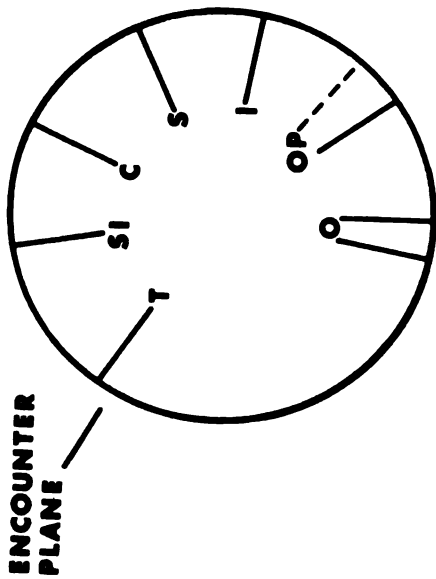
Another limit on eruptive launch regions is established by photographic evidence which strongly suggests that relatively undisrupted crust underlies the region between Mare Oriental and the western edge of Oceanus Procellarum (Plate 3). Launching of lunar subsurface material, then, is not permitted here.

To demonstrate that the flyby encounter model is viable, it must be shown that the primary backfall pattern described above can be derived from the Oceanus Procellarum and/or Mare Oriental volcanic eruptive launch regions under reasonable encounter parameters. Reasonable encounter velocities are from 0-10 km/sec; closest approach distances must be within the W limit, but not less than  $1.3 R_e (C_m - C_e)$ .

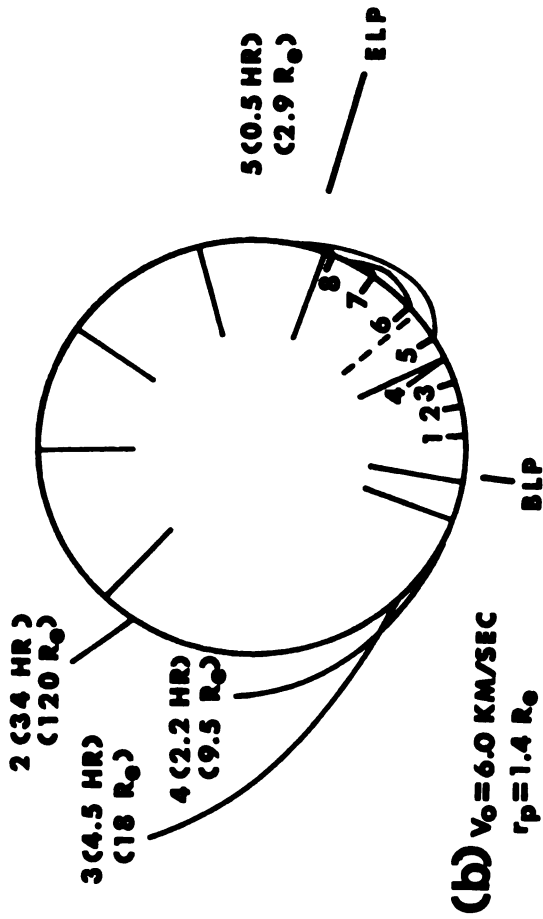
Since the primary ejection and backfall features lie nearly on a great circle on the lunar surface, they can be projected onto a great-circle cross section with little distortion. Figure 6a shows such a section in which the central location of the circular maria and the limits of both Mare Oriental and the inferred initial eruptive launch center of Oceanus Procellarum are indicated.

Figure 6.--Geometrical comparison of model and actual lunar surface patterns.

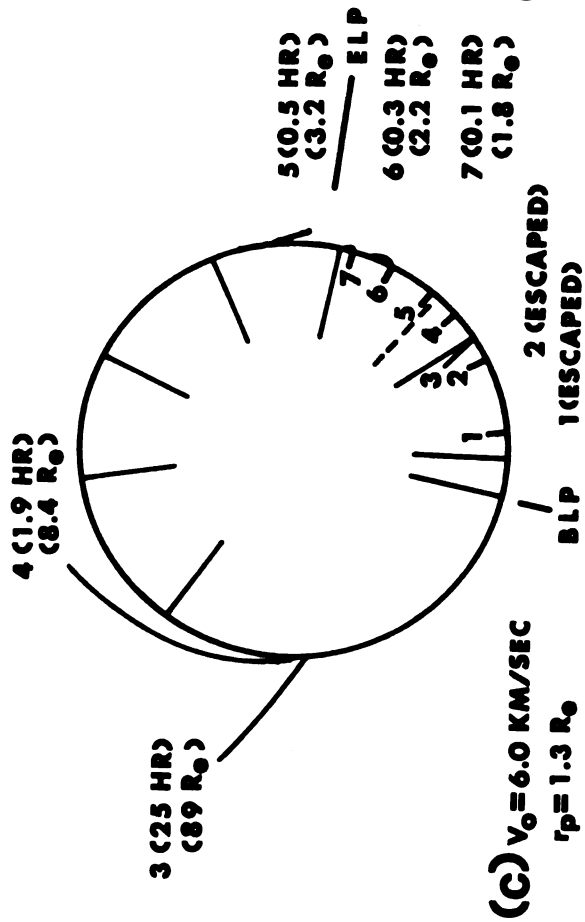
(a) Cross-sectional diagram of Moon showing geometrical location of lunar surface features which lie nearly on a great circle. Launch phase features: O = Mare Oriental; angular extent about  $10^\circ$ ; OP = Oceanus Procellarum; broken line located about  $15^\circ$  from western edge; eastern edge of OP grades into Mare Imbrium. Backfall phase features (lines point to center of feature): I = Mare Imbrium; S = Mare Serenitatis; C = Mare Crisium, SI = Mare Smythii; T = Mare Tsiolkovsky. Angular distances: O (center to T) =  $240^\circ$ ; O (center to OP (western edge)) =  $40^\circ$ ; OP (western edge) to I (center) =  $45^\circ$ ; I to S =  $35^\circ$ ; S to C =  $40^\circ$ ; C to SI =  $35^\circ$ ; SI to T =  $45^\circ$ . (b) Superimposition of geometry of lunar features onto geometry of model flyby encounter from Figure 4. (c) Superimposition of geometry of lunar features onto geometry of lunar flyby encounter with same  $V_0$  (= 6.0 km/sec) but with  $r_p = 1.3 R_e$  (0.1  $R_e$  closer to Earth). Launch sites, flight times, and distances of Moon from Earth ( $C_m-C_e$ ) at time of impact are given for bodies 1-7. (d) Diagram similar to (c) with several additional launch sites located between launch sites 4 and 6. Note that all bodies launched between sites 5 and 6a form a concentrated impact pattern; those launched between sites 4 and 5 form a much more dispersed impact pattern.



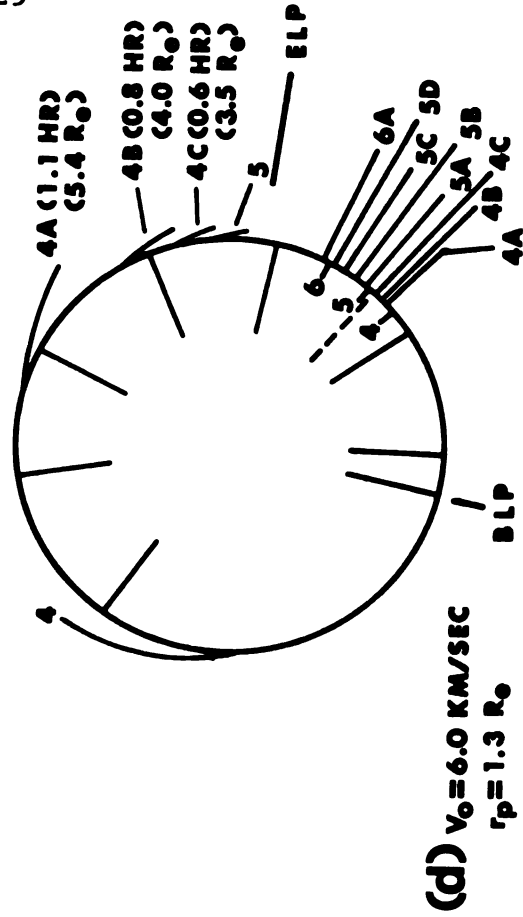
(a)



(b)  $v_0 = 6.0 \text{ KM/SEC}$   
 $r_p = 1.4 R_0$



(c)  $v_0 = 6.0 \text{ KM/SEC}$   
 $r_p = 1.3 R_0$



(d)  $v_0 = 6.0 \text{ KM/SEC}$   
 $r_p = 1.3 R_0$

Figure 6b shows the major properties of the theoretical model from Figure 4 superimposed onto the geometry of lunar features. This diagram shows that all materials ejected between launch points 4 and 6 will fall back within the general region of the large circular maria.

Figure 6c shows a slightly modified version of Figure 6b in which the closest approach distance is decreased to  $1.3 R_e$ , encounter velocity remaining constant. Such a change shifts the launching activities counterclockwise relative to the geometry of the Moon. This makes it possible, under ideal conditions, to derive all mare basalts for the primary pattern of the backfall phase from between launch points 4 and 6, a section of lunar surface that is located entirely within Oceanus Procellarum.

Figure 6d is based on the same encounter parameters as Figure 6c but shows additional launch points in critical locations. This diagram shows that there is a contrast in density distribution of impact sites, although the launch sites are nearly uniformly distributed. This pattern of dispersion of backfall features away from the source should be characteristic of flyby encounter products and should be detectible in the resulting backfall patterns.

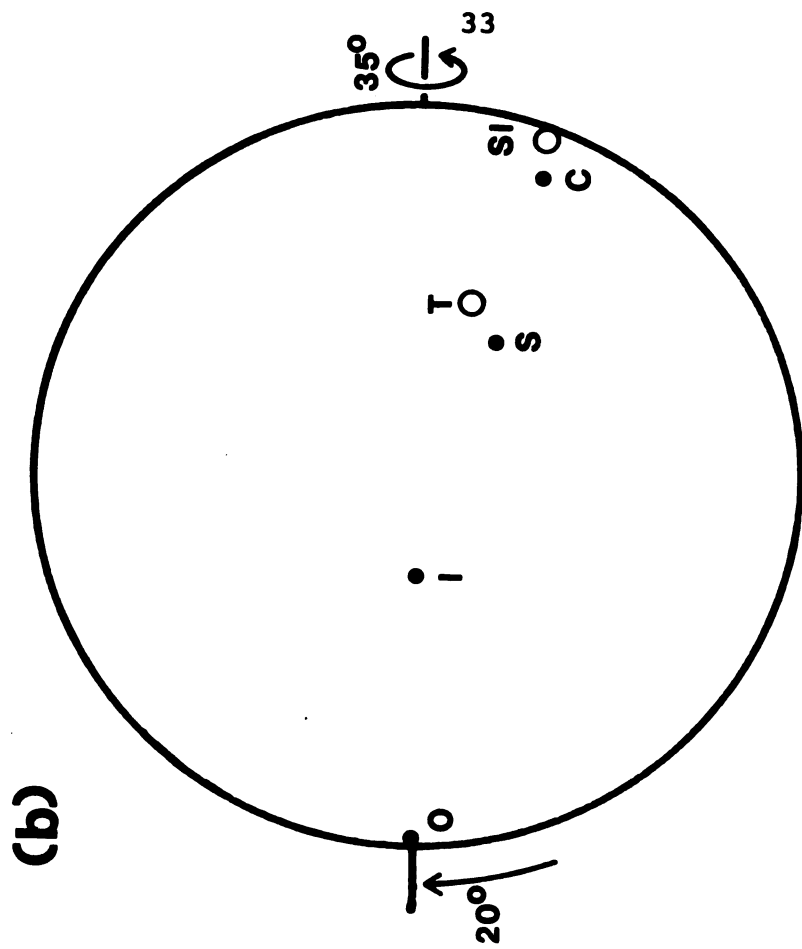
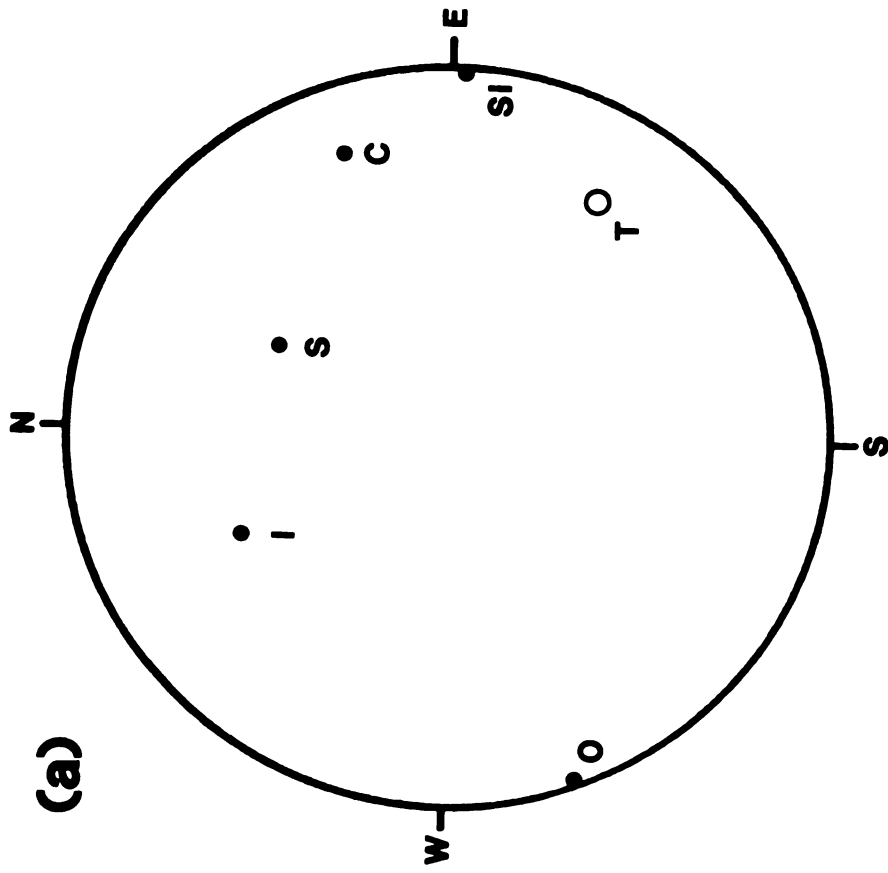
The geometric models presented in Figure 6 imply that, under those encounter conditions, all material launched from the Mare Oriental region would escape from the Moon. Thus, using these models, the materials from Mare Oriental would not be associated with the backfall pattern.

It is necessary, then, to obtain all backfalling material for the line of circular maria, which were delineated as part of the backfall phase, from the Oceanus Procellarum source region. Furthermore, all launching must occur within about  $30^\circ$  to  $40^\circ$  of arc between the western edge of Oceanus Procellarum and the eastern edge of Mare Imbrium. These restrictions are considered to be firm geometric constraints that must be satisfied by any viable encounter model. Although it is not a unique solution, the model presented in Figure 6d with  $V_o = 6.0$  km/sec and  $r_p = 1.3 R_e$  satisfies these geometric constraints. The placing of limits on possible encounter parameters that are consistent with the geometric constraints listed above is beyond the scope of this paper.

Relative to the position of the paleospin poles during the proposed flyby encounter, map-view locations of actual lunar features are pertinent. Figure 7a shows the present positions of the centers of the maria located on the curvilinear pattern of the large circular maria shown in Figure 6 and Plate 1. Figure 7b shows the positions of these features after reorientation of Mare Oriental to the BLP position of Figure 5. Comparison of the pattern in Figure 7b to patterns in Figures 5d and f suggests that the paleospin poles, during the encounter, were located at some position intermediate to those in Figures 5d and f. Determination of a more exact location is beyond the scope of this work.

Figure 7.---(a) Map-view diagram (orthographic projection) of Moon showing the location of major surface features which lie nearly on a great circle. Symbols are identical to those in Figure 6. (b) Map-view diagram of Moon showing the location of lunar surface features after clockwise rotation of  $20^\circ$  and north to south rotation of front face  $35^\circ$ . This orientation corresponds to that in the model rotation diagrams in Figure 5 with Mare Oriental located at the BLP (begin launch phase position).





In this section, features on the real lunar surface, which are compatible with those that could be generated during a flyby encounter, have been outlined. The major backfall phase features consist of a curvilinear pattern of circular maria which generally decrease in diameter away from the source. Their occurrence as individually distinct features implies that their progenitors departed from the source region as individual bodies (spheroids) of lunar basalt and travelled as coherent bodies above the lunar surface to the impact site. Upon impact, they bent down the lunar crust and collapsed upon themselves to form circular lava lakes (maria) on the lunar surface.

Details of the Rock Pattern.--The encounter model can furnish explanations for the origin and development of lunar surface features in various amounts of detail. Certain features are predictable, whereas others are merely compatible with the model. As examples of the value of this model for explanation and prediction, salient properties of two major lunar surface features, Mare Imbrium and Mare Crisium, will be analyzed.

The Development of Mare Imbrium.--In this encounter model, the development of large circular maria on the lunar surface is the result of the backfall of molten or partially molten basaltic spheroids. The results of such an event would be dependent primarily on the flexibility of the lunar crust and secondarily on the viscosity of the impacting

body. If the lunar crust had been inflexible, a basaltic spheroid would have impacted and splattered over a large area. If the crust had been thin and if molten material had existed a short distance below, then a spheroid would have most likely penetrated the crust and blended in with the molten material below. If the crust had been somewhere between these extremes, a lunar basaltic spheroid would have depressed the crust on impact and collapsed upon itself. Then, some of the material from the spheroid most likely would have rolled out onto the edges of the crustal depression and finally come to rest at the lowest elevation possible. The most prominent surface feature to be produced in the latter case would have been a lava lake (mare) occupying an indentation produced by the impact of the spheroidal body that carried the material to the lake.

The formation of the Imbrium System (Mutch, 1970) can be explained by this general process of backfalling basaltic materials. Figure 6d shows that all materials ejected between launch sites 5 and 6 would fall back within the general vicinity of Mare Imbrium. Whether the basin was formed by the impact of a group of bodies or by one large basaltic body is not important here. In either case a great excess of basaltic materials would be concentrated at this location. After collapse of the basaltic body or bodies, a tsunami-like wave of molten lunar basalts would be expected to spread out in a radial pattern over the raised rim of the newly formed Imbrium basin and

to flood the surrounding terrain. This can be visualized, in geologic terms, as a gigantic transgression of mare basalts over the primitive crust of the Moon. After the maximum extent of transgression (in the case of Imbrium, the system of features stretches over 1000 km. from the basin center), the basaltic lavas that were still molten would have sought the lowest level available, and thus would have flooded any depressions in the transgressed region. Plate 4 shows a typical view of the final state after the regressive phase.

The regressive activity would have been characterized by continuous crystallization at the liquid basalt-solid material interface and, in effect, would have "covered the tracks" of this gigantic cycle of transgression and regression. The most diagnostic product of such a flood of mare basalts would have been the production of a great volume of breccias with sedimentary-like bed forms and flow structures. Unlike normal sedimentary rocks, the flowing medium (basalt) would have formed the matrix of the resulting breccia and the clasts would have been remnants of the transgressed surface, in most cases the primordial crust of the Moon. Such breccias have been recovered from the Fra Mauro Formation, a formation which can be predicted by the encounter model to show these features quite prominently. Likewise, the cross-stratification observed on the wall of Hadley Rille and on the walls of Mount Hadley (Apollo Lunar Investigation Team,



Plate 4.--Photograph of typical example of flooded terrae. Location of photo is shown in Plate 1 (southern edge of Sinus Medii). Lineation of features, NW-SE. Buried and flooded craters are evidence of overprint of older terrain by younger material. Low albedo of some materials suggests that they are of basaltic composition, similar to that of the major maria. Secondary craters (post-flooding) apparently represent the latest event to affect the area. (Lunar Orbiter Photograph IV 101 H3).

1972) on the Apollo 15 mission, is probably some of these sedimentary bed forms and cross-beds associated with the drainage of mare basalts from the Appenine Mountains following the tsunami-like wave activities. In other words, these breccias and bed forms were most likely associated with the post-flood readjustment or runoff period. Subsequently, these particular cross-beds were probably exhumed by faulting.

The Development of Mare Crisium.--Mare Crisium is an example of a mare which probably resulted from the impact of a single basaltic spheroid. This particular mare was chosen because (1) it is isolated from the other maria and (2) it displays all the features of both larger and smaller circular maria, such as a raised rim and the secondary cratering on both its mare and rim surfaces.

The diagram in Figure 6d suggests that the spheroids forming the major circular maria should have impacted at a relatively low angle to the lunar surface. Inspection of Mare Crisium (Plate 5) shows that it does indeed have an elliptical outline and that the eastern part of the mare shows generally shallower features than the western part.

Under conditions of the encounter outlined in Figure 6c and 6d, some of the first materials ejected from the Procellarum center could have had trajectories which would have returned them to the lunar surface at various times following the encounter. This material, then, could have been responsible for secondary cratering of mare

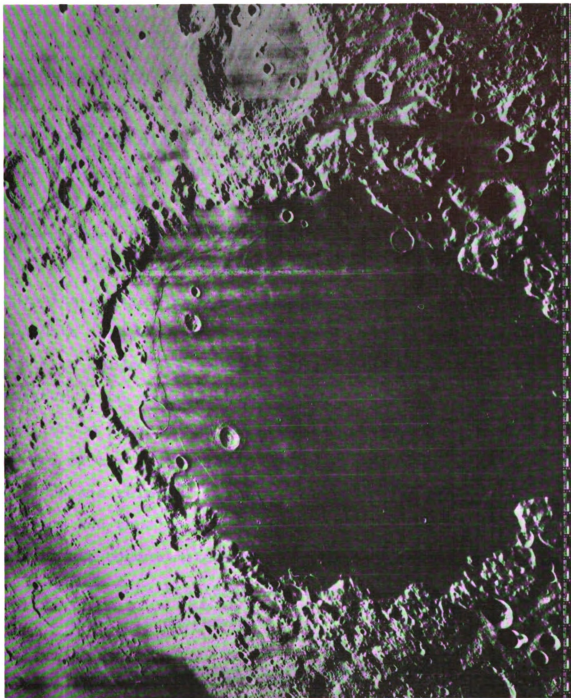


Plate 5.--Photograph of Mare Crisium, a typical circular Mare, showing raised rim, flooded terrae on edge, and various stages in the development of secondary (post-mare) cratering. (Lunar Orbiter Photograph IV 191 H3).

surfaces shortly after their emplacement. However, for a crater to result from particle impact, the mare surface must be an effective crater counter, i.e., it must be able to preserve the "scar."

Relating this to Mare Crisium, it can be assumed, from previous discussions, that Crisium's rim was mantled with basaltic mare material at the time of emplacement of the mare basalts. The mare edges (Plate 5) have many more superimposed craters than the mare surface itself, and the edge of the mare surface has many more secondary craters than its central portion. This morphological evidence suggests that most of the secondary impacts occurred while the mare surface was molten and still an ineffective crater counter. The absence of secondary craters, of a size similar to those found near the edges, near the central region of the mare strongly suggests that the secondary impacts are related, in time, to the origin of the mare surface and thus to the flyby encounter event itself, and not to subsequent meteoritic impacts. A further implication is that very little has happened to the Mare Crisium region since its emplacement.

Predictions Based on the Model.--This model for the origin of mare and mare-related rocks predicts certain features that could be tested on future missions to the Moon. Some of these predictions are consistent with data already recovered from lunar surface materials.



1. There should be no primitive crust under the Mare Oriental and Oceanus Procellarum eruptive launch regions outlined on Plates 1 and 3.

2. The major circular maria should be saucer-shaped deposits of lunar basalts which are underlain by primitive crust. The central depths of these circular maria should be proportional to their diameters and should be on the order of 10's of kilometers. The observable mass concentrations (mascons) should be a very small proportion of the mare volumes.

3. After isotopic distribution anomalies are accounted for, all mare and mare-related materials that were melted during the encounter should give about the same radiometric age. This should be about 3.6 billion years. The breccias should be notable exceptions. They should give a blended age of their respective components.

4. The most deformed crustal regions on the Moon should lie along the encounter plane. The major deformation features should occur as broadscale corrugations of the crust trending perpendicular to the encounter plane. On the other hand, the least deformed regions should lie near the poles of the encounter plane. These effects can be tested by both laser beam altimeter and crater ellipticity studies on the primitive crust.

### Model Effects on Earth

The major effects on the Earth resulting from a lunar flyby encounter within the W limit would be heating of the upper mantle region by tidal friction mechanisms. The magnitude of this heating would be dependent on the physical state of the Earth's upper mantle at the time of encounter. Quantitative treatment of the heating effects on the Earth (and Moon) are beyond the scope of this paper. However, qualitatively, the effects can be described as follows: If the Earth were highly deformable at this time, then high amplitude lithospheric tides would occur incident to the encounter. Consequently, great amounts of heat energy would be generated within the Earth's primitive crust and upper mantle during the raising and dissipation of these tides. On the contrary, if the Earth were rigid and relatively undeformable (much like its present condition), then only low amplitude lithospheric tides would develop and very little heat would be absorbed by the Earth per encounter.

The combined action of high lithospheric tides and the resulting heat dissipation would lead to widespread disruption of the Earth's primitive crust. The reaction of the crust-upper mantle rock system would be to re establish dynamic (physical and chemical) equilibrium. This would be accomplished by gradual processes in which the old crust would be subducted at places of mantle current descent and a new, thinner crust, which would be more in equilibrium with the new heat regime of the upper mantle,

would be generated at mantle rises. In broad view, this can be considered as an accelerated process of sea-floor spreading.

In summary, then, the two planets, Earth and Moon, would react quite differently to a lunar flyby encounter. The Earth's upper mantle would possess a quantity of heat sufficient to "heal over" encounter scars, whereas the smaller body would probably not.

#### Comparison to the Rock Record on Earth

Recent syntheses of isotopic ratios in rocks and minerals (Patterson and Tatsumoto, 1964; Steuber and Murthy, 1966; Hurley, 1968; and others) and rock and mineral dates and other evidence summarized by Cloud (1968, 1972) suggest to Cloud that the Earth underwent a major event about  $3.5 \pm 3.6$  billion years ago. This event, apparently thermal in nature, seemingly affected the Earth's crust and upper mantle on a planet-wide scale. Evidence of such an event, although tenuous at our present state of knowledge, is congruent with the theoretical predictions of what could occur during a very close lunar flyby encounter with a primitive Earth. This problem deserves further study.

## CHAPTER III

### IMPLICATIONS FOR THE HISTORY OF THE EARTH-MOON ASSOCIATION

Interpretation of the pattern of large circular maria as flyby encounter "scars" implies that the Moon's orbital history can be divided into three general eras: heliocentric asteroidal orbital era, heliocentric Earth-crossing orbital era, and geocentric orbital era. Using the statistical calculations of Gerstenkorn (1969), some broad limits can be placed on the time scale of these eras. Gerstenkorn considered the fate of an asteroid that was perturbed into an Earth-crossing orbit by Jupiter; the asteroid's aphelion at this point was 2.8 A. U. He estimated that, on the average, this orbit could exist only  $1-5 \times 10^8$  years; then it would be changed by an encounter the closest approach distance of which would be equal to or less than  $1.4 R_e$ . Then within  $0.5-1.0 \times 10^9$  years, and after many encounters, Gerstenkorn estimates that a collision with Earth would probably occur. In addition, he shows that encounters with Mars would not change this time scale significantly.

This work of Gerstenkorn, combined with evidence of a flyby encounter of the Moon with the Earth about 3.6 billion years ago, suggests a time scale for the evolution of the Earth-Moon System outlined in Figure 8.

Evidence of one flyby encounter implies a series of such encounters over a period of geologic time with the Moon during at least one of these passing well within the weightlessness limit. The first sufficiently strong interaction between Earth and Moon would have broken Jupiter's control over the asteroid-Moon's orbit and practically insured an Earth-Moon association of collision or capture (Gerstenkorn, 1969; Alfven and Arrhenius, in press). Subsequently, each sufficiently close lunar flyby encounter would have transformed orbital kinetic energy into planetary heat energy through tidal friction mechanisms. Then during a long period of time and many flyby encounters, the asteroid-Moon's orbit would have shrunk into a near Earth-coincident orbit from which a capture could have been executed.

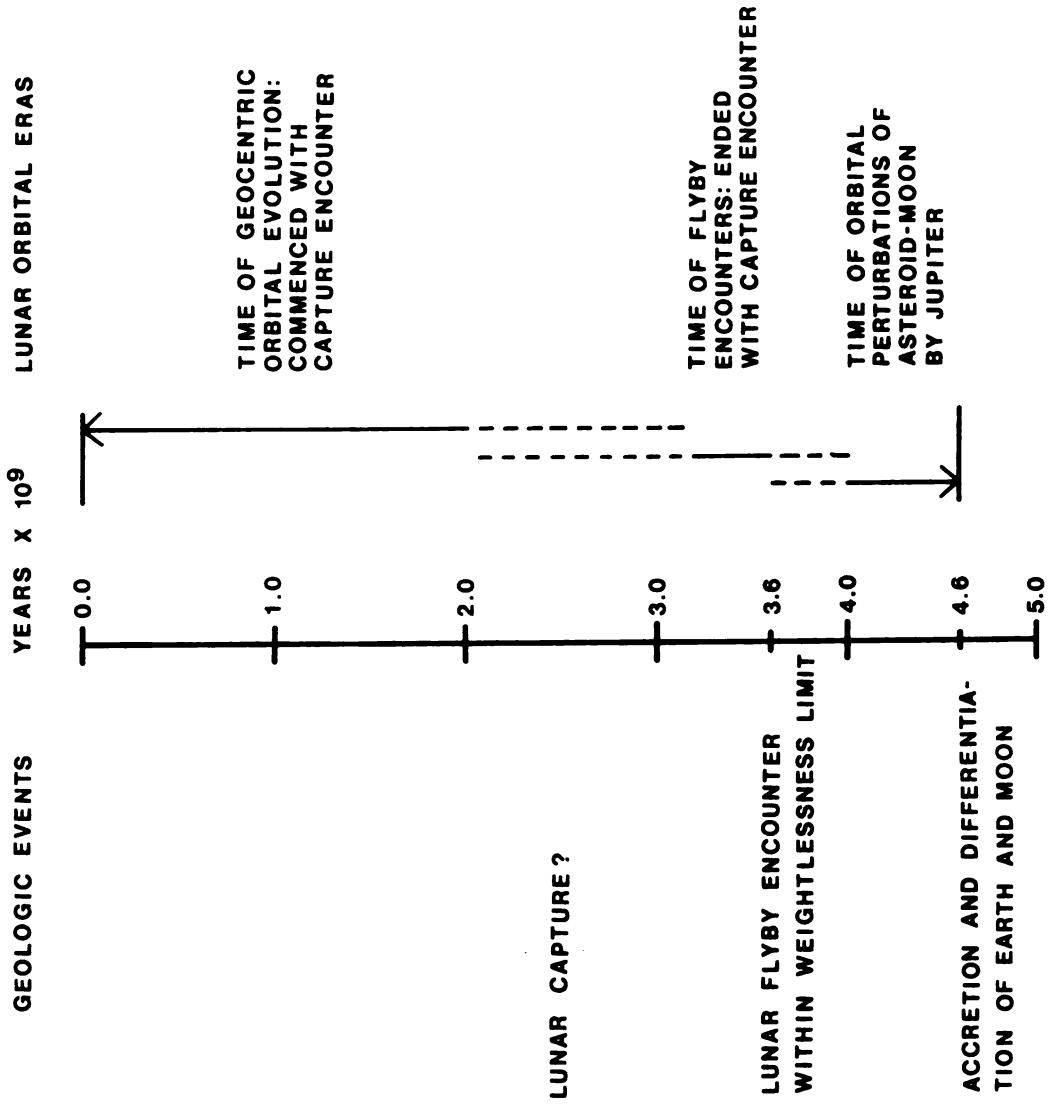


Figure 8.--Time scale for the evolution of the Earth-Moon System.

## CHAPTER IV

### SUMMARY AND CONCLUSIONS

In summary, the physical consequences of lunar flyby encounters were analyzed using computer simulation techniques. It was found that the weightlessness limit of the Earth-Moon System (located at  $1.63 R_e$ ,  $C_e - C_m$ ) was of major physical importance. In this model, transport of a substantial mass of lunar crust and lunar upper mantle material could result only (1) if an encounter was well within the weightlessness limit and (2) if the lunar upper mantle could yield large quantities of magma over a very short period of time (20-30 minutes) while within this weightlessness limit.

Comparison of the actual lunar surface pattern, mainly outlined by the geometric pattern of circular maria, to the simulation model pattern shows that they are compatible. The large circular maria are thought to be the impact locations of large spheroidal, lunar basaltic masses which were launched from a region of Oceanus Procellarum and transported above the lunar surface by an interaction of Earth and Moon gravitational forces to impact positions during the launch and backfall phases of a single lunar

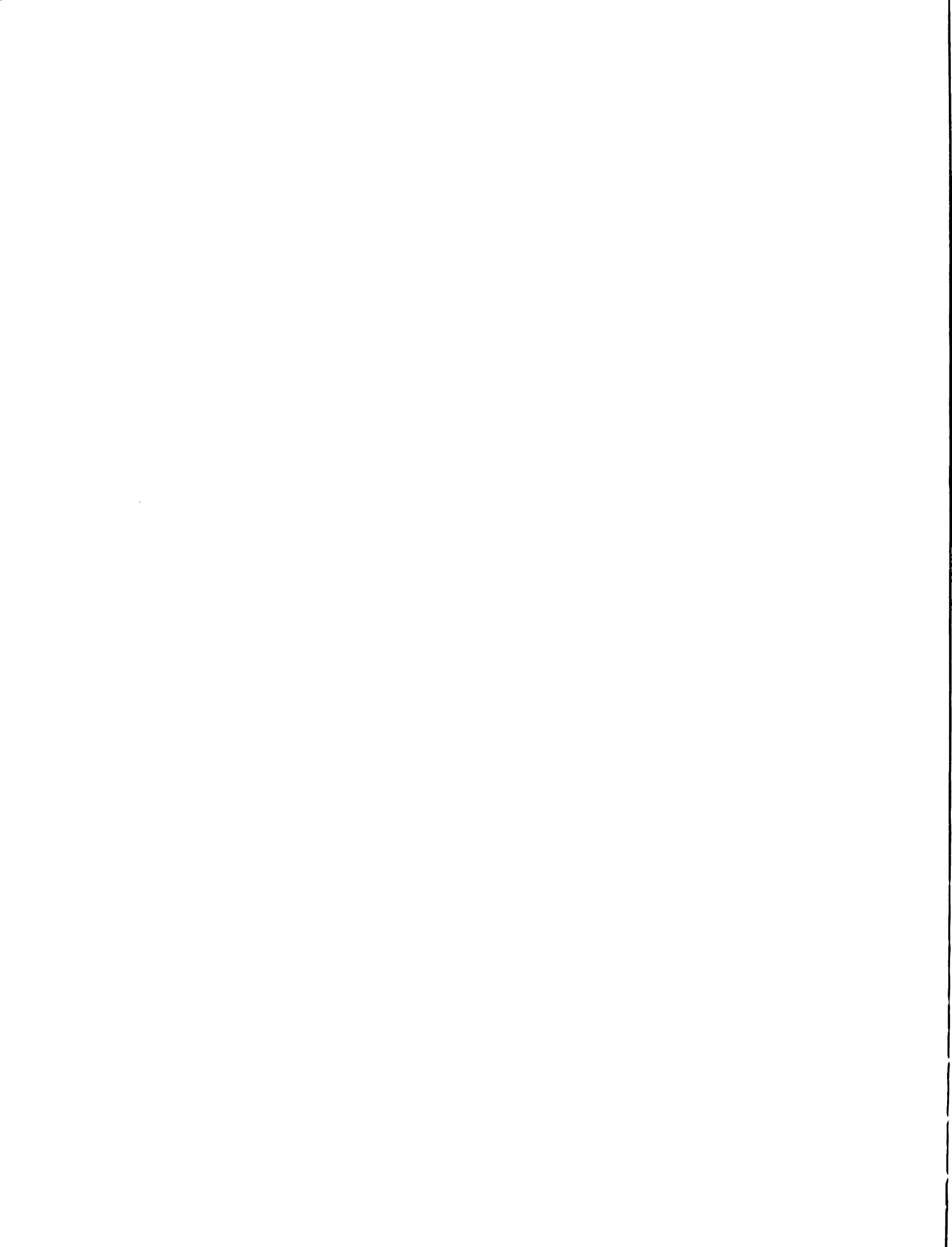
flyby encounter. Upon impact these spheroidal masses simultaneously bent down a pliable lunar crust, collapsed upon themselves, and formed large circular lava lakes (maria) on the lunar surface. Photographic evidence of such a pattern can be used to place limits on physical conditions of the encounter, as well as on petrologic and physical conditions of the lunar body itself. Comparison of the position of lunar surface features to a set of geometrical constraints shows that it is compatible with that of an encounter whose  $V_0 = 6.0$  km/sec and  $r_p = 1.3 R_e$ . However, this is not a unique solution but only one of a family of solutions whose limits have not yet been determined. In general, the pattern implies that launching of magmatic material was discontinuous and that the bulk of the maria basalts were launched during the latter stage of the launch phase. Whether more than one such encounter is recorded on the lunar surface is an open question.

Evidence from both the Moon and Earth of a flyby encounter about 3.6 billion years ago, combined with Gerstenkorn's (1969) statistical calculations for the case of an asteroid in Earth-crossing orbit, can be used to outline three broad lunar orbital eras during which the lunar body was transferred from its place of origin within the Asteroid Belt to its present location in geocentric orbit.



#### REFERENCES CITED

- Alfven, H. and Arrhenius, G. 1970a. Structure and evolutionary history of the Solar System, I: *Astrophys., Space Sci.*, v. 8, p. 338-421.
- \_\_\_\_\_, 1970b. Origin and evolution of the Solar System, II: *Astrophys., Space Sci.*, v. 9, p. 3-33.
- \_\_\_\_\_. 1973. Origin and evolution of the Earth-Moon System: *The Moon*, v. 5, in press.
- Apollo Lunar Geology Investigation Team. 1972. Geologic setting of the Apollo 15 samples: *Science*, v. 175, p. 407-415.
- Baldwin, R. B. 1966. On the origin of the Moon: *Jour. Geophys. Res.*, v. 71, p. 1936-1937.
- Birch, F. 1965. Speculations on the Earth's thermal history: *Geol. Soc. America Bull.*, v. 76, p. 133-154.
- Cloud, P. E. 1968. Atmospheric and hydrospheric evolution on the primitive Earth: *Science*, v. 160, p. 729-736.
- \_\_\_\_\_. 1972. A working model of the primitive Earth: *Am. Jour. Sci.*, v. 272, p. 537-548.
- Darwin, G. H. 1898. *The tides and kindred phenomena in the Solar System*: (reprinted in 1962) Freeman and Co., 378 p.
- Gerstenkorn, H. 1969. The earliest past of the Earth-Moon System: *Icarus*, v. 11, p. 189-207.
- Hanks, T. C., and Anderson, D. L. 1969. The early thermal history of the Earth: *Phys. Earth Planet. Interiors*, v. 2, p. 19-29.
- Hinners, N. W. 1971. The new Moon: a view: *Reviews Geophys. Space Phys.*, v. 9, p. 447-521.
- Hurley, P. M. 1968. Absolute abundance and distribution of Rb, K and Sr in the Earth: *Geochim. Cosmochim. Acts*, v. 32, p. 273-283.



- Kaula, W. M. 1971. Dynamical aspects of lunar origin: Reviews Geophys. Space Phys., v. 9, p. 217-238.
- Lowman, P. D. 1972. The geologic evolution of the Moon: Jour. Geol., v. 80, p. 125-166.
- Mutch, T. A. 1970. The geology of the Moon: Princeton Univ. Press, 324 p.
- Patterson, C. and Tatsumoto, M. 1964. The significance of lead isotopes in detrital feldspar with respect to chemical differentiation within the earth's mantle: Geochim. Cosmochim. Acta, v. 28, p. 1-22.
- Ringwood, A. E. 1960. Some aspects of the thermal evolution of the Earth: Geochim. Cosmochim. Acta, v. 20, p. 241-259.
- \_\_\_\_\_. 1966. The chemical composition and origin of the Earth, in Hurley, P. M., ed., Advances in earth science: Mass. Inst. Tech. Press, p. 287-356.
- \_\_\_\_\_. 1969. Composition and evolution of the upper mantle, in Hart, P. J., ed., The Earth's crust and upper mantle: Am Geophys. Union Mon. 13, p. 1-17.
- Ruskol, E. L. 1966. On the past history of the Earth-Moon System: Icarus, v. 5, p. 221-227.
- Singer, S. F. 1968. The origin of the Moon and geophysical consequences: Geophys. Jour., Royal Astron. Soc., v. 15, p. 205-226.
- Smith, J. V., Anderson, A. T., Newton, R. C., Olsen, E. J., and Wyllie, P. J. 1970. A petrologic model for the Moon based on petrogenesis, experimental petrology, and physical properties: Jour. Geol., v. 78, p. 381-405.
- Sonett, C. P., Colburn, D. S., Dyal, P., Parkin, C. W., Smith, B. F., Schubert, G., and Schwartz, K. 1971. Lunar electrical conductivity profile: Nature, v. 230, p. 359-362.
- Steuber, A. M. and Murthy, V. R. 1966. Strontium isotope and alkali element abundances in ultramafic rocks: Geochim. Cosmochim. Acta, v. 30, p. 1243-1259.
- Wood, J. A. 1972. Thermal history and early magmatism in the Moon: Icarus, v. 16, p. 229-240.

MICHIGAN STATE UNIV. LIBRARIES



31293010057051